Supporting information

Nanoscale ion emitters in native mass spectrometry for measuring ligand-protein binding affinities

Giang T. H. Nguyen,[†] Thinh N. Tran,[‡] Matthew N. Podgorski,[§] Stephen G. Bell,[§] Claudiu T. Supuran[ǁ] and William A. Donald[*,†]

[†] *School of Chemistry, University of New South Wales, Sydney, NSW, 2052, Australia*
[‡] *School of Electrical Engineering and Telecommunications, University of New South Wales, Sydney, NSW, 2052, Australia*
[§] *Department of Chemistry, University of Adelaide, Adelaide, 5005, Australia*
[ǁ] *University of Florence, Department of Neuroscience, Psychology, Drug Research and Child's Health, Section of Pharmaceutical and Nutraceutical Sciences, Via Ugo Schiff 6, 50019, Sesto Fiorentino, Italy*

Table of contents

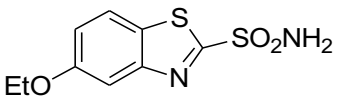

Ethoxzolamide – L_1

(258)

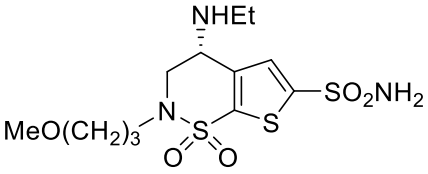

Brinzolamide – L_2

(383)

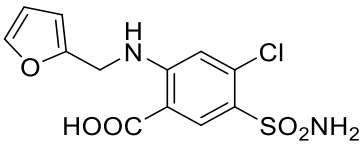

Furosemide – L_3

(330)

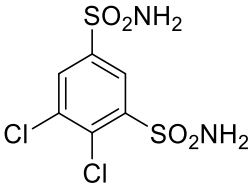

Dichlorophenamide – L_4

(305)

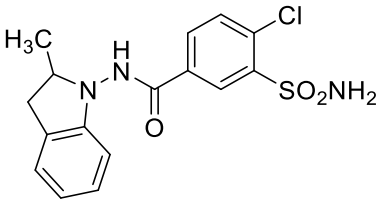

Indapamide – L_5

(365)

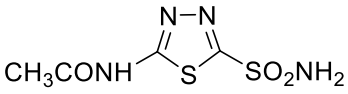

Acetazolamide– L_6

(222)

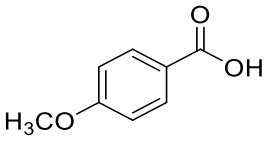

4-methoxybenzoic acid – L_7

(152)

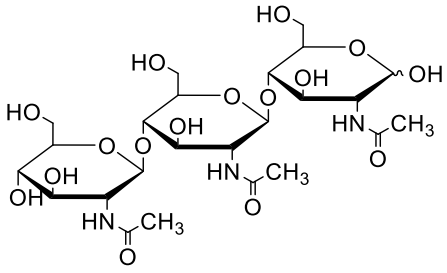

Tri-N-acetylchitotriose – L_8

(627)

Scheme S1. Structures of the ligands used in native mass spectrometry experiments. The molecular weight of each ligand (in Da) is shown in parentheses.

Table S1. Ligand concentrations that were analysed to obtain the K_d values of ligands to human carbonic anhydrase I and lysozyme that are reported in Figure 1 and Table 1. Solutions containing 5 μM protein, 70 mM ammonium acetate, and each concentration of ligand were measured in triplicate by native MS to obtain an average K_d value (Figure 1 and Table S2).

Ligand	Concentration (μM)
Ethoxzolamide	1, 2, 3, 4
Brinzolamide	1, 2, 3, 4, 8
Furosemide	1, 2, 3, 4
Dichlorophenamide	1, 2, 3, 4
Indapamide	1, 3, 5, 10, 15
Acetazolamide	1, 2, 3, 4
Tri-N-acetylchitotriose	3, 7, 10, 15

Table S2. K_d (μM) values measured using nanoelectrospray ionization mass spectrometry and emitter tips with different inner diameters.

Protein-Ligand	Inner diameter of emitter tip				Literature
	250 nm	500 nm	850 nm	2000 nm	
hCAI-L_1	0.014 ± 0.002	0.015 ± 0.002	0.018 ± 0.003	0.024 ± 0.004	0.009[1], 0.025[2]
hCAI-L_2	1.06 ± 0.05	1.12 ± 0.07	1.13 ± 0.11	1.70 ± 0.15	0.73[a]
hCAI-L_3	0.055 ± 0.005	0.053 ± 0.005	0.058 ± 0.006	0.079 ± 0.009	0.062[3]
hCAI-L_4	1.3 ± 0.1	1.3 ± 0.1	1.5 ± 0.1	1.9 ± 0.2	1.2[4]
Lys-L_8	7.6 ± 0.1	7.9 ± 0.2	7.8 ± 0.2	9.4 ± 0.3	6.6[5], 8.6[6], 9.9[7], 11.1[8]

[a]This work; value was measured using a CA inhibition assay.

Table S3. CYP199A4 was produced recombinantly using *Escherichia coli* and purified using standard biological buffers and protein chromatography techniques.[9]

Sequence	VSNSSAESISAPPNDSTIPHLAIDPFSLDFFDDPYPDQQTLRDAGPVV YLDKWNVYGVARYAEVHAVLNDPTTFCSSRGVGLSDFKKEKPWRPP SLILEADPPAHTRPRAVLSKVLSPATMKTIRDGFAAAADAKVDELLQR GCIDAIADLAEAYPLSVFPDAMGLKQEGREHLLPYAGLVFNAFGPPN ELRQTAIERSAPHQAYVNEQCQRPNLAPGGFGACIHAFTDTGEITPD EAPLLVRSLLSAGLDTTVNGIGAAVYCLARFPGELQRLRSDPTLARNA FEEAVRFESPVQTFFRTTTREVELGGAVIGEGEKVLMFLGSANRDPR RWSDPDLYDITRKTSGHVGFGSGVHMCVGQLVARLEGEVMLSALAR KVAAIDIDGPVKRRFNNTLRGLESLPVKLTPA
Length	409 amino acids
Mass	Average mass: 44392 Da Protein mass plus heme (616.5 Da): 45008.5 Da

Methods

Fabrication of nano- and micro-scale nanoelectrospray ionization emitters.

Nanoelectrospray ionization emitters with different tip diameters were fabricated in-house from borosilicate glass capillaries (Harvard Apparatus, 1.2-mm o.d., 0,68-mm i.d.) using a microcapillary puller (Model P-97, Sutter Instruments, Novato, CA, USA) using the parameters listed in Table S4. Approximately 30 emitters were sequentially fabricated within 30 min, and stored in a petri dish on double stick tape under ambient conditions. For reproducibility, all emitters that were used in all reported ESI-MS and SEM experiments were fabricated and coated on the same day using the same heating filament for the tip puller. The inner diameters of the ion emitters depend strongly on the tip pulling conditions (Table 4) and the position of the heating filament. Each batch of 30 emitters were sputter coated together simultaneously with a mixture of gold and palladium (Scancoat Six, Edwards, UK). The nanoscale ion emitters can be stored for at least 6 months prior to use if care is taken not to break the tips. For the narrowest bore ion emitters, it is important to ensure that any air bubble(s) do not block the ESI solution from reaching the tip orifice. For example, approximately 3 in 10 of the 250 nm ion emitters were blocked by an air bubble, such that ESI-MS signal for protein ions could not be measured. The air bubbles could be identified using a microscope camera (WAT-704R, Watec, Japan). Shaking the emitters vigorously side-to-side by hand can be used to remove the air bubble(s) in some instances.

Table S4. Tip puller conditions used to fabricate nanoelectrospray ionization emitters.

Parameter	~ 250 nm	~ 500 nm	~ 850 nm	~ 2000 nm
Heat	535	535	535	535
Pull	70	60	30	0
Velocity	80	60	30	20
Time	-	-	250	250
Delay	1	1	-	-
Pressure	500	500	500	500

CA catalytic activity and ligand-binding assay.

We used a stopped-flow spectrophotometer instrument (Sx.18Mv-R Applied Photophysics, Oxford, UK) for measuring the CA catalyzed CO_2 hydration activity between hCAI and brinzolamide.[10] Stock solutions of hCAI and ligand were prepared at 100 μM each in distilled-deionized water and diluted with the buffer (0.2 mM phenol red, 10 mM Hepes pH 7.4 and 10 mM Na_2SO_4) to the desired concentration. The concentration of hCAI was fixed at 0.1 μM and a variable amount of ligand was added. Protein and ligand solutions were preincubated together for 15 min at room temperature prior to the assay in order to form the complex. Phenol red working at the absorbance maximum of 557 nm was used as indicator. The rate of CO_2 hydration was measured by tracking the pH change as a result of the formation of hydronium ions using the change in the absorbance of the indicator. The inhibition constants were obtained by non-linear least-squares methods using the Cheng-Prusoff equation[11] from the average of at least three replicates.

General equation for obtaining dissociation constants (K_d) in native MS.

For each mass spectrum, peak areas corresponding to the unbound and ligand-bound protein were automatically integrated by an inhouse software program entitled PLbinding, which was written in MATLAB (2017a, The MathWorks, Natick, MA). The code for this software is available in the supporting materials as a separate file owing to the length of the script. This software was also used to calculate the K_d values for single or multiple ligands competing for binding at a single binding site of a target protein.

Consider a protein (*P*) with a single ligand-binding site for a total of *i* different ligands (L_i), where *i* is an integer (Equation S1).

$$PL_i \overset{K_{d,i}}{\longleftrightarrow} P + L_i \quad \text{(S1)}$$

The K_d value for the dissociation equilibrium (Equation S1) for each ligand is defined as,

$$K_{d,i} = \frac{[P][L_i]}{[PL_i]} \quad \text{(S2)}$$

where $[P]$, $[L_i]$, and $[PL_i]$ are the concentrations of the unbound protein, unbound ligand, and the protein-ligand complexes, respectively. The initial concentrations of the ligand(s) ($[L_i]_0$) and protein ($[P]_0$) are given by Equations S3 and S4, respectively.

$$[L_i]_0 = [L_i] + [PL_i] \quad \text{(S3)}$$

$$[P]_0 = [P] + \sum_i [PL_i] \quad \text{(S4)}$$

If the relative concentrations of the bound and unbound protein complexes in solution are the same as the relative abundances in the gas phase, then: (i) the initial protein concentration in solution is proportional to the sum of the integrated abundances of the

unbound protein ion charge states ($\sum_n P^{n+}$) and that of the bound protein ion charge states ($\sum_i \sum_n PL_i^{n+}$; Equation S5); (ii) the concentration of the unbound protein in solution is proportional to $\sum_n P^{n+}$ (Equation S6); and (iii) the concentration of the bound protein ion complexes are proportional to $\sum_n PL_i^{n+}$ (Equation S7).

$$[P]_0 \propto \sum_n P^{n+} + \sum_i \sum_n PL_i^{n+} \quad \text{(S5)}$$

$$[P] \propto \sum_n P^{n+} \quad \text{(S6)}$$

$$[PL_i] \propto \sum_n PL_i^{n+} \quad \text{(S7)}$$

Thus, the ratios between the concentration of the unbound protein to the initial concentration of protein (Equation S8) and the ratio between the concentrations of the protein-ligand complexes and the initial protein concentration (Equation S9) can be readily obtained from the abundances of the protein ions and protein-ligand complex ions.

$$\frac{[P]}{[P]_0} = \frac{\sum_n P^{n+}}{\sum_n P^{n+} + \sum_i \sum_n PL_i^{n+}} \quad \text{(S8)}$$

$$\frac{[PL_i]}{[P]_0} = \frac{\sum_n PL_i^{n+}}{\sum_n P^{n+} + \sum_i \sum_n PL_i^{n+}} \quad \text{(S9)}$$

By combining Equations S3 and S9, the unbound ligand concentration can be obtained (Equation S10).

$$[L_i] = [L_i]_0 - \frac{\sum_n PL_i^{n+}}{\sum_n P^{n+} + \sum_i \sum_n PL_i^{n+}} [P]_0 \quad \text{(S10)}$$

By substituting $[P]$, $[PL_i]$, and $[L_i]$ in Equation S2 with Equations S8, S9 and S10, the Equation S11 (Equation 1 in main text) is obtained, which can be used obtain $K_{d,i}$ values

directly from the abundances of the protein and protein-ligand complex ions in ESI mass spectra.

$$K_{d,i} = \frac{\sum_n P^{n+}}{\sum_n PL_i^{n+}}\left([L_i]_0 - \frac{\sum_n PL_i^{n+}}{\sum_n P^{n+} + \sum_i \sum_n PL_i^{n+}}[P]_0\right) \quad \text{(S11)}$$

For K_d measurements in solutions with high concentrations of salt, the top four most abundant salt adducted protein ions without the ligand bound, $[P,nNa,zH]^{(n+z)+}$, and those with the ligand bound, $[PL,nNa,zH]^{(n+z)+}$, were integrated across all charge states to obtain the values for $\sum_n P^{n+}$, and $\sum_n PL_i^{n+}$.

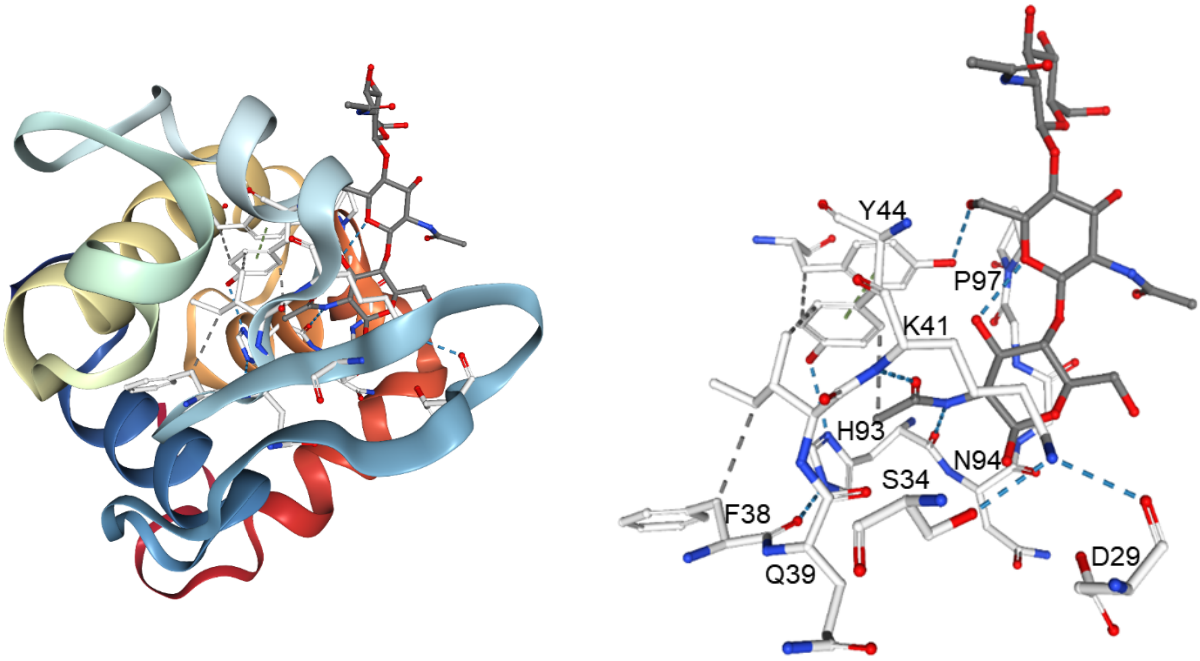

Figure S1. Hen egg-white lysozyme co-crystallized with the Tri-N-acetylchitotriose (gray) (PDB code 3AB6).[12]

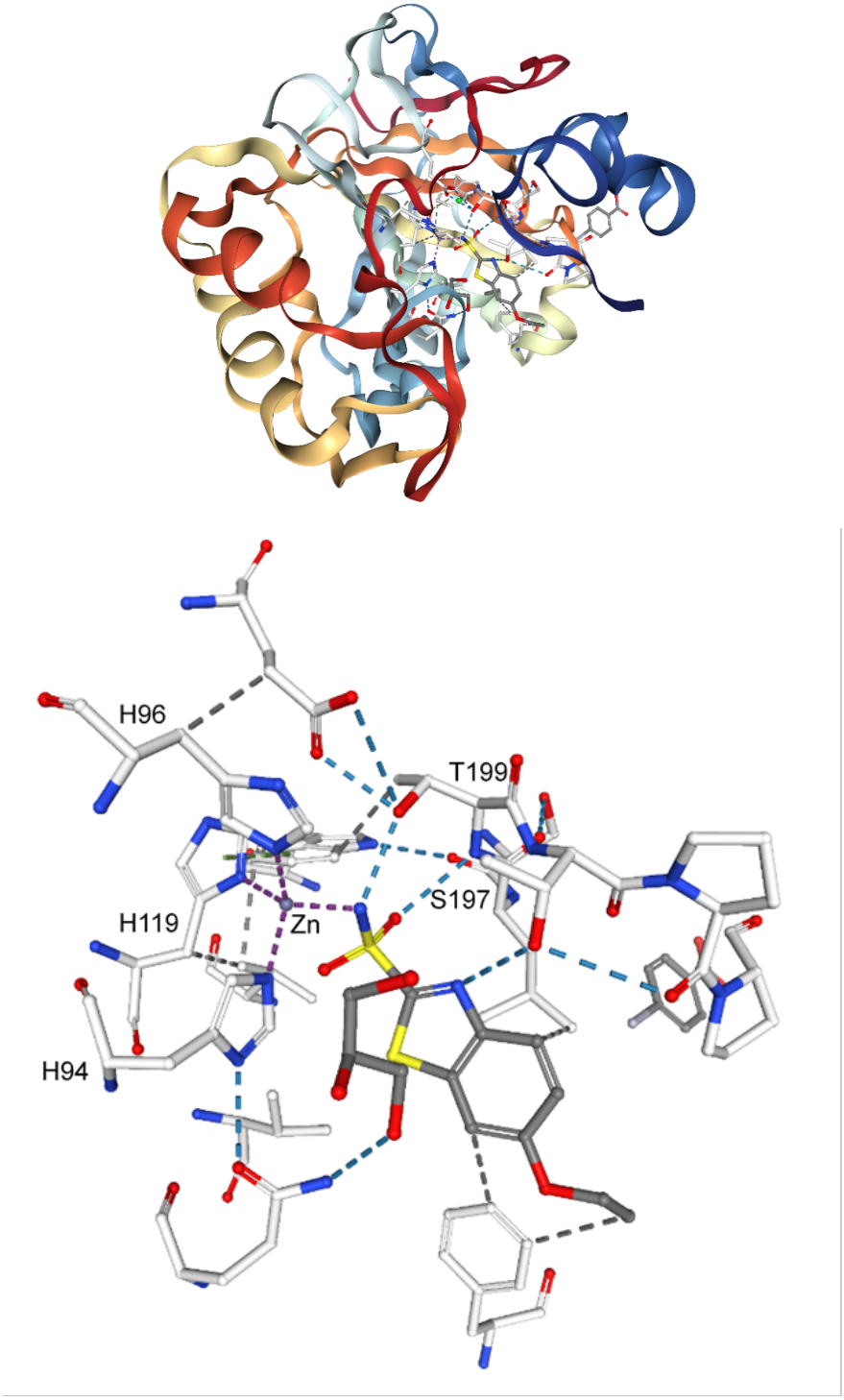

Figure S2. Carbonic anhydrase II co-crystallized with the ethoxzolamide (gray) (PDB code 3CAJ).[13]

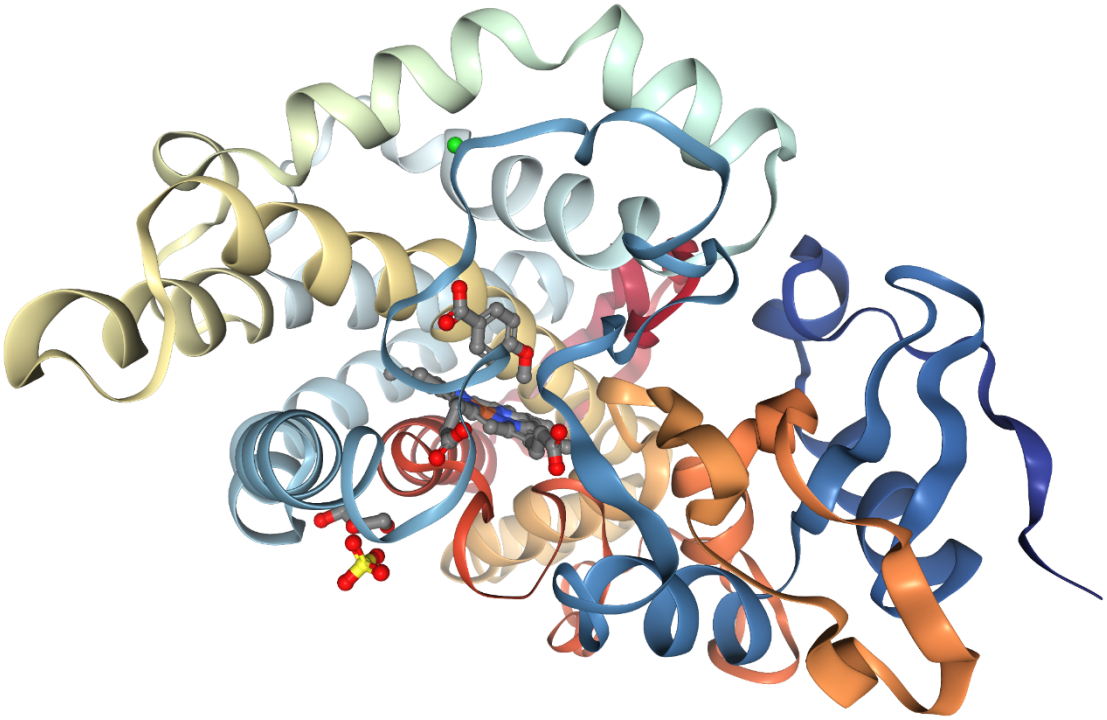

Figure S3. CYP199A4 co-crystallised with 4-methoxybenzoic acid (PDB code 4DO1).[14]

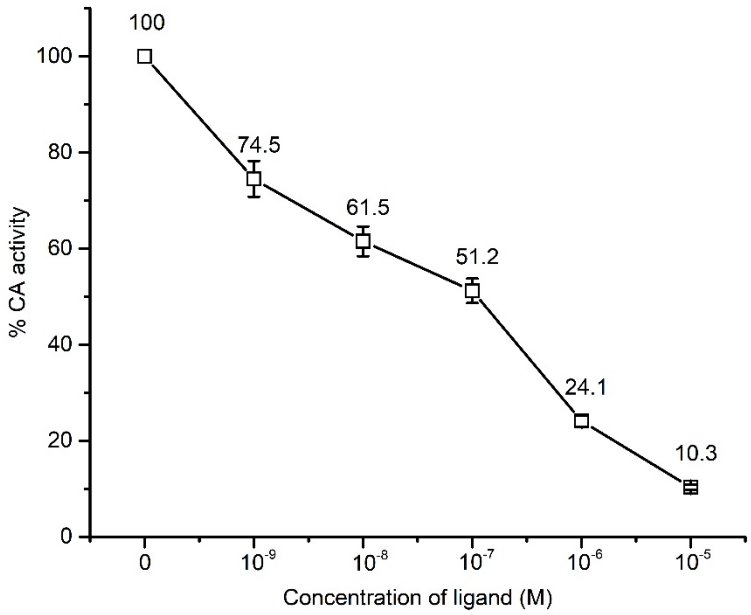

Figure S4. The extent of catalytic activity of human carbonic anhydrase I for 1.0×10^{-7} M human carbonic anhydrase I as a function brinzolamide concentration (1.0×10^{-5} to 10^{-9} M) in 20 mM Hepes pH 7.4 and 10 mM Na_2SO_4 using CA catalytic activity and ligand-binding assay.

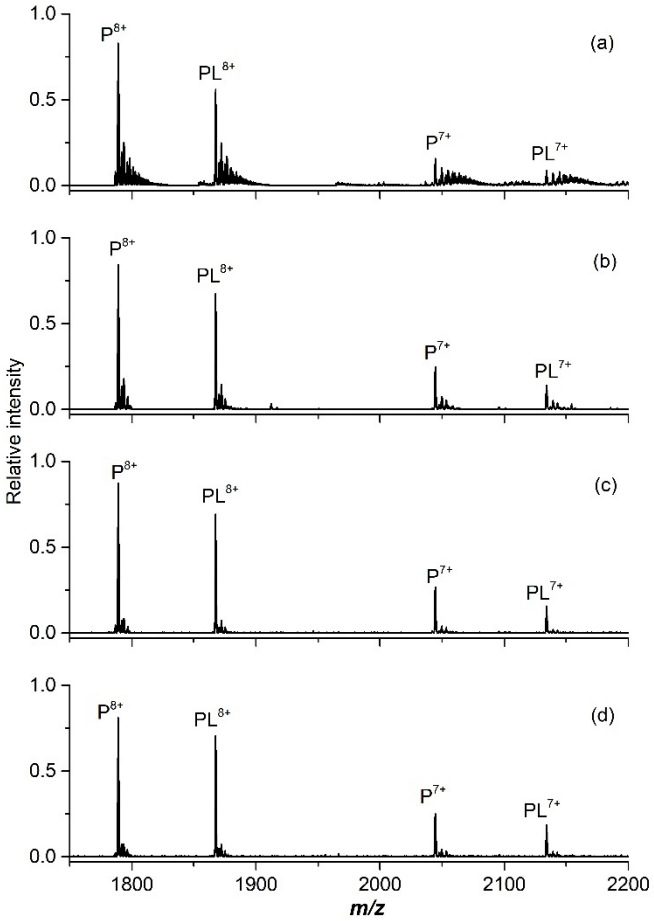

Figure S5. Nanoelectrospray ionization mass spectra of 5 μM Lysozyme and 7 μM tri-N-acetychitotriose in 70 mM aqueous ammonium acetate (pH 7.4) using emitter tips with inner diameters of (a) ~2000 nm, (b) ~850 nm, (c) ~500 nm, and (d) ~250 nm.

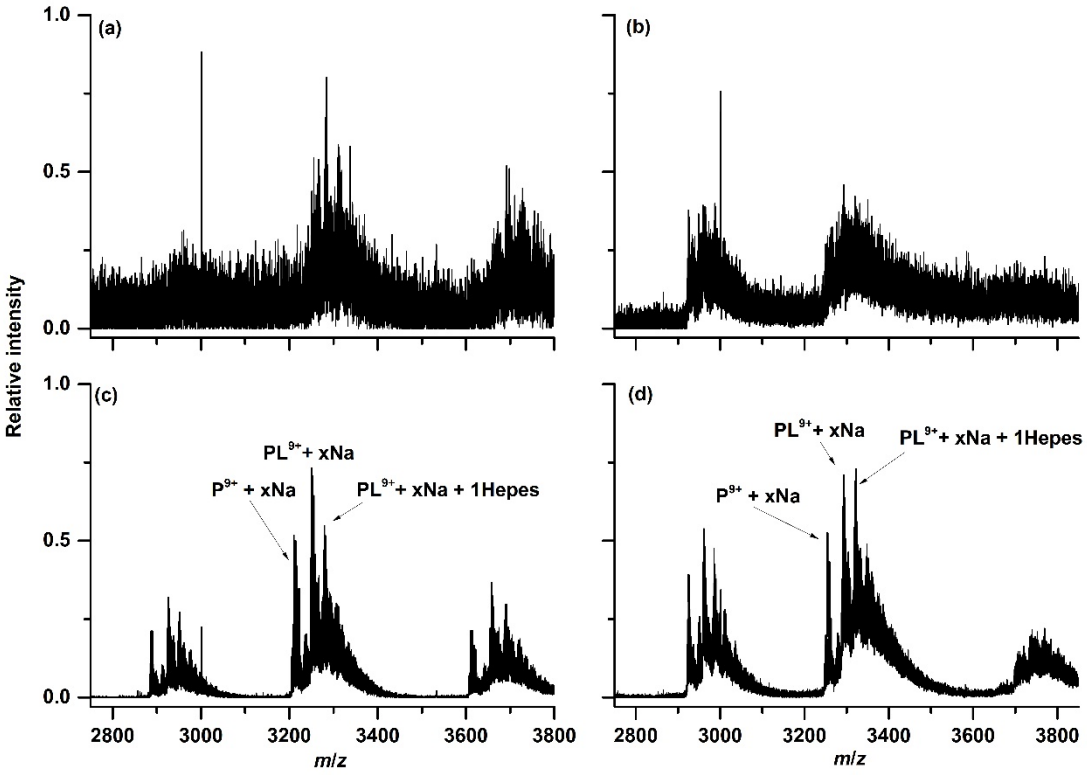

Figure S6. Nanoelectrospray ionization mass spectra of (a,c) hCAI in complex with brinzolamide, and (b,d) hCAII with indapamide in 10 mM Hepes and 10 mM sodium sulfate pH 7.4 using emitter tips with inner diameters of (a,b) ~2000 nm emitter tips, and (c,d) ~250 nm.

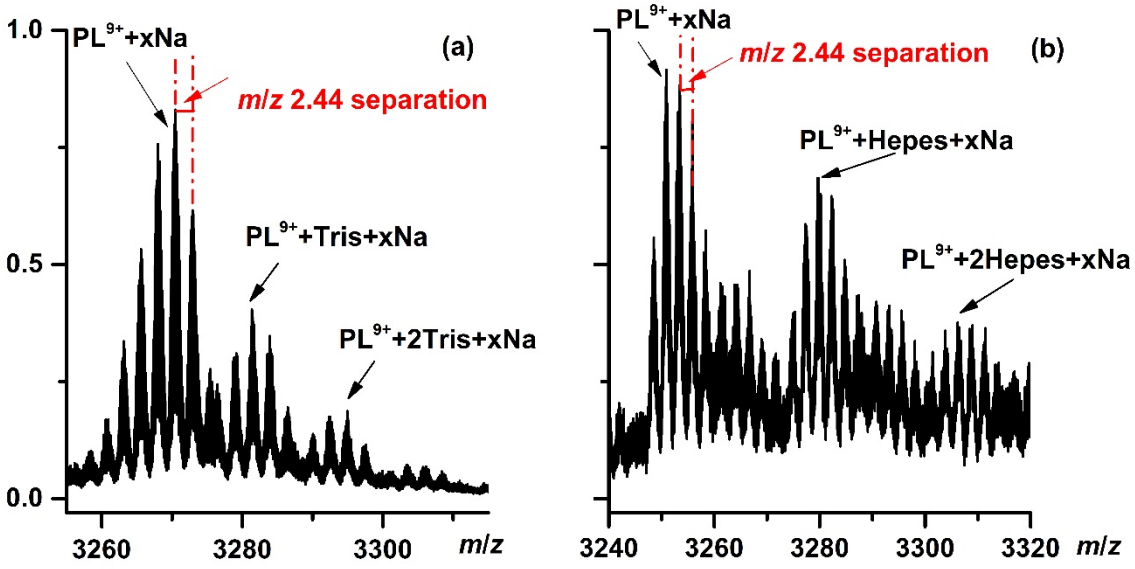

Figure S7. Nanoelectrospray ionization mass spectra of the 9+ charge states of (a) human carbonic anhydrase I and brinzolamide formed from aqueous 50 mM NaCl and 20 mM Tris-HCl buffer (pH 7.4); and (b) human carbonic anhydrase II and indapamide from aqueous 10 mM Hepes and 10 mM Na_2SO_4. The peaks separated by an *m*/*z* spacing of 2.44 corresponds to the adduction of sodium ions to the protein ion complexes; i.e. $\Delta m/z$ = (22.90 - 1.01)/9 = 2.44 (replacement of a proton with a sodium cation).

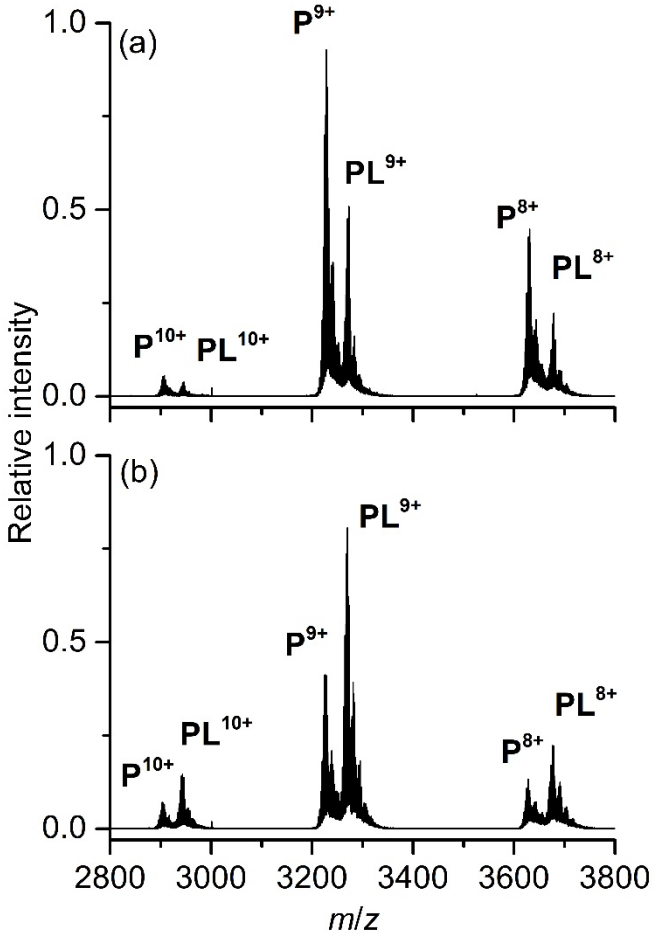

Figure S8. Nanoelectrospray ionization mass spectra of 5 μM human carbonic anhydrase I with (a) 1 μM brinzolamide, and (b) 3 μM brinzolamide aqueous 50 mM NaCl and 20 mM Tris-HCl buffer (pH 7.4) using emitter tips with inner diameters of ~250 nm.

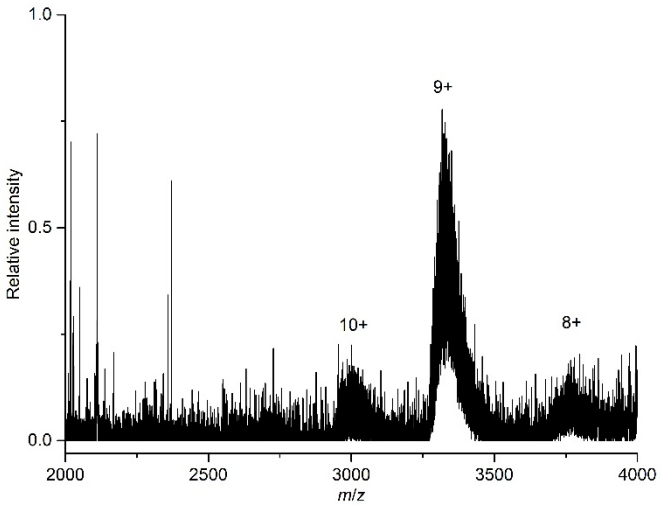

Figure S9. Nanoelectrospray ionization mass spectra of hCAII in complex with indapamide in aqueous 150 mM NaCl and 20 mM Tris-HCl pH 7.4.

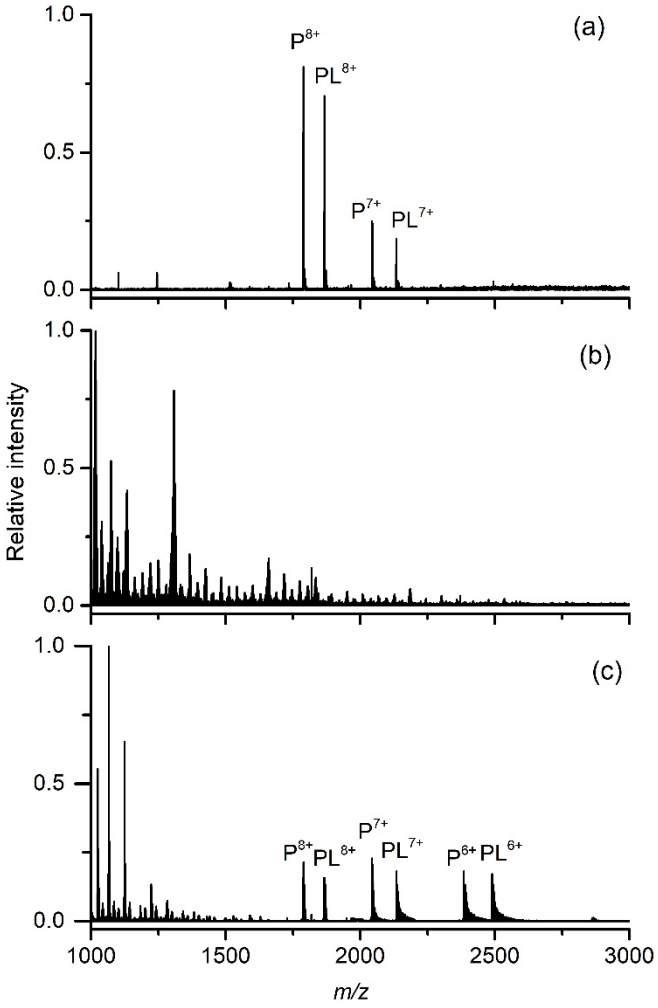

Figure S10. Nanoelectrospray ionization mass spectra of 5 μM lysozyme and 7 μM Tri-N-acetylchitotriose (L_8) in aqueous (a) 70 mM ammonium acetate buffer pH 7.4 and (b,c) 50 mM NaCl and 20 mM Tris-HCl buffer pH 7.4 using emitter tips with inner diameters of (b) ~2000 nm, and (a,c) ~250 nm.

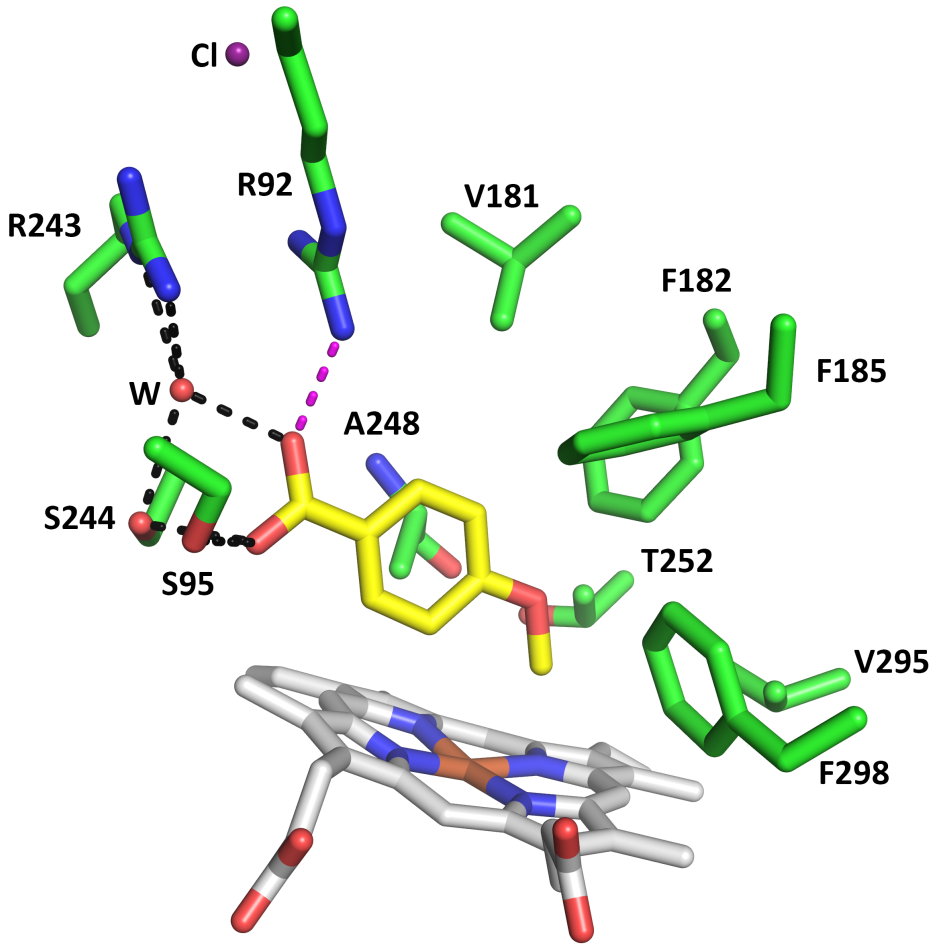

Figure S11. 4-methoxybenzoic acid bound in the active site of CYP199A4 (PDB code: 4DO1). Active site residues are depicted in green, the heme in grey, 4-methoxybenzoic acid in yellow and the chloride ion in purple. The water molecule which interacts with 4-methoxybenzoic acid is shown as a red sphere. Hydrogen bonds are represented by black dashed lines. A salt bridge between R92 and the substrate carboxylate is represented by a pink dashed line.[14]

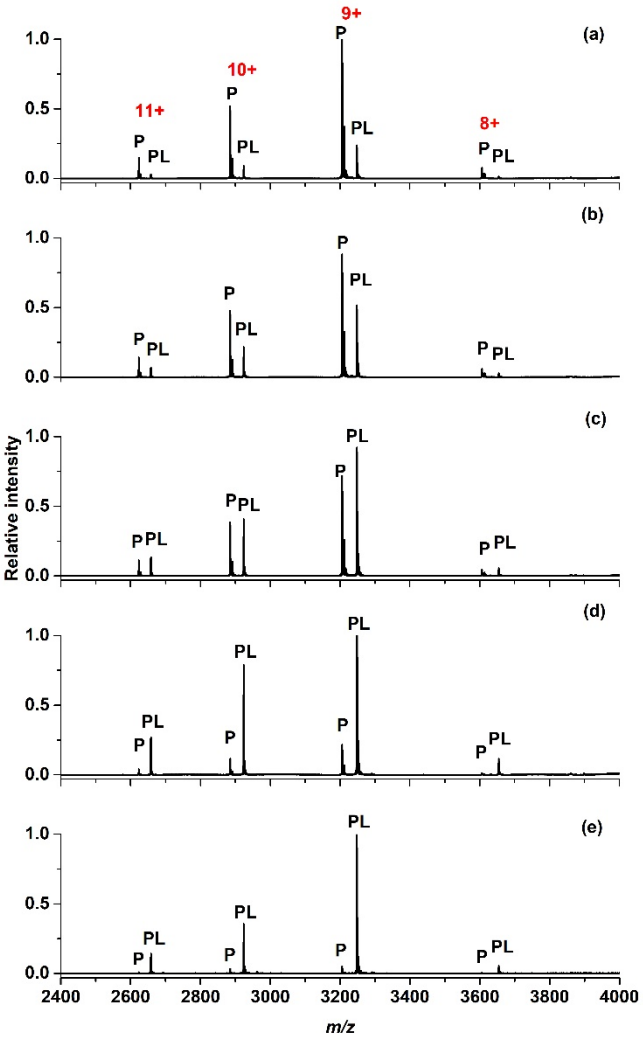

Figure S12. Nanoelectrospray ionization mass spectra of hCAI and brinzolamide in 70 mM ammonium acetate (pH 7.5) using ~250 nm emitter tips with different ratios of protein and ligand: (a) 5:1, (b) 5:2, (c) 5:3, (d) 5:4 and (e) 5:8.

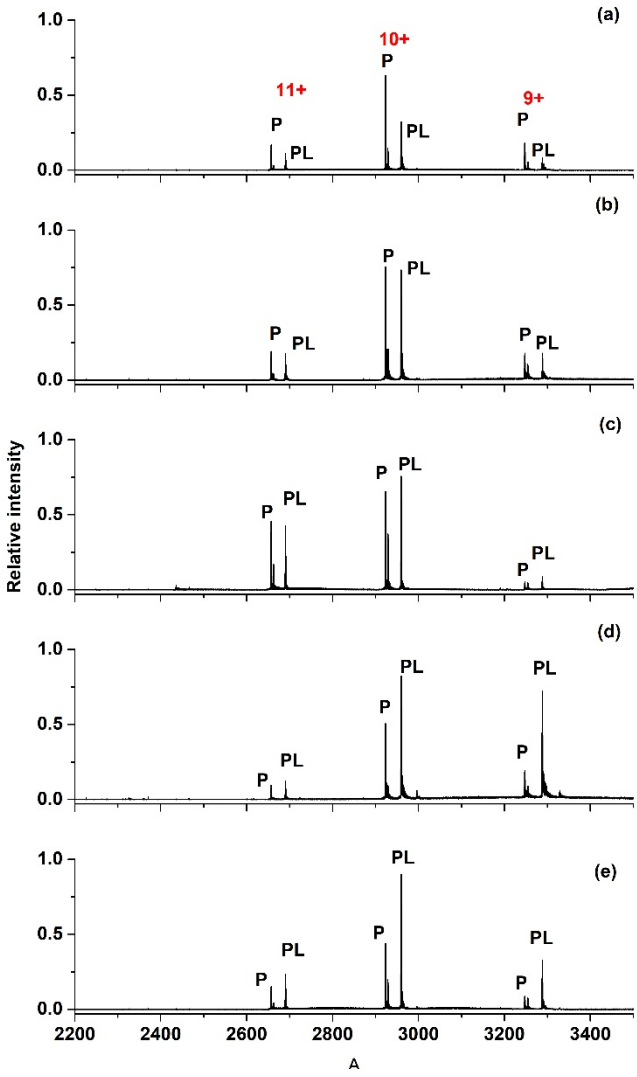

Figure S13. Nanoelectrospray ionization mass spectra of hCAII and indapamide in 70 mM ammonium acetate (pH 7.5) using ~250 nm emitter tips with different ratios of protein and ligand: (a) 5:1, (b) 5:3, (c) 5:5, (d) 5:10 and (e) 5:15.

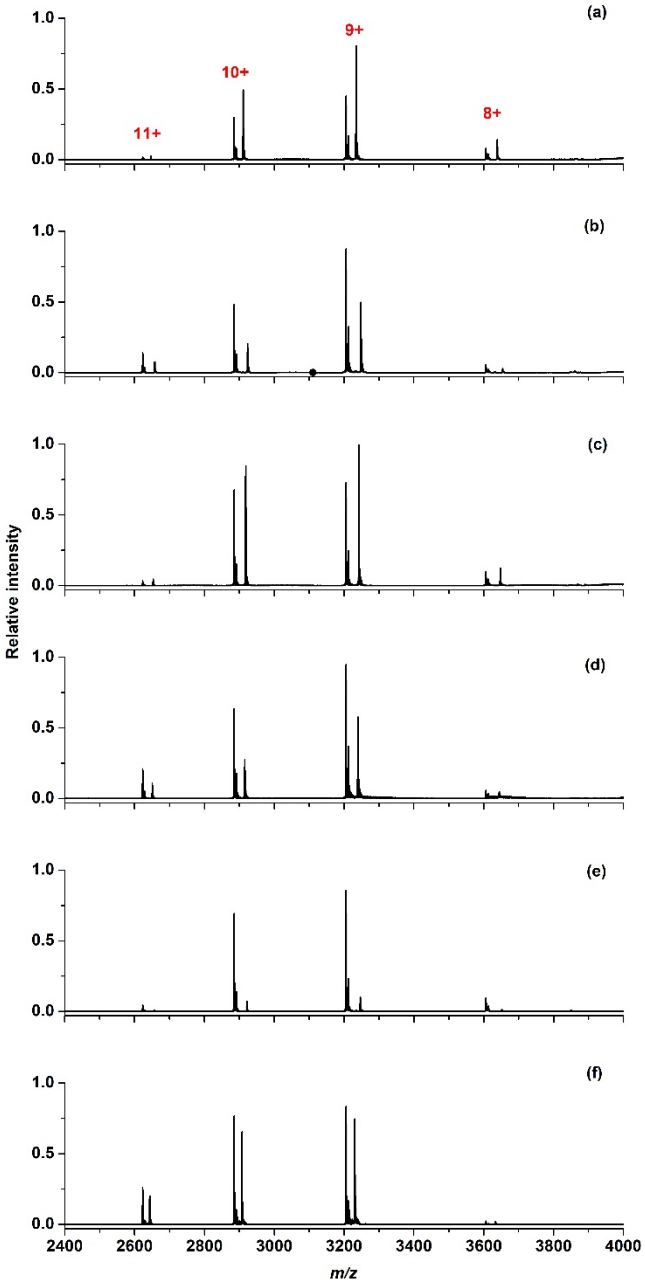

Figure S14. Nanoelectrospray ionization mass spectra of human carbonic anhydrase I and (a) ethoxzolamide, (b) brinzolamide, (c) furosemide, (d) dichlorophenamide, (e) indapamide and (f) acetazolamide in aqueous 70 mM ammonium acetate (pH 7.4) using ~250 nm emitter tips

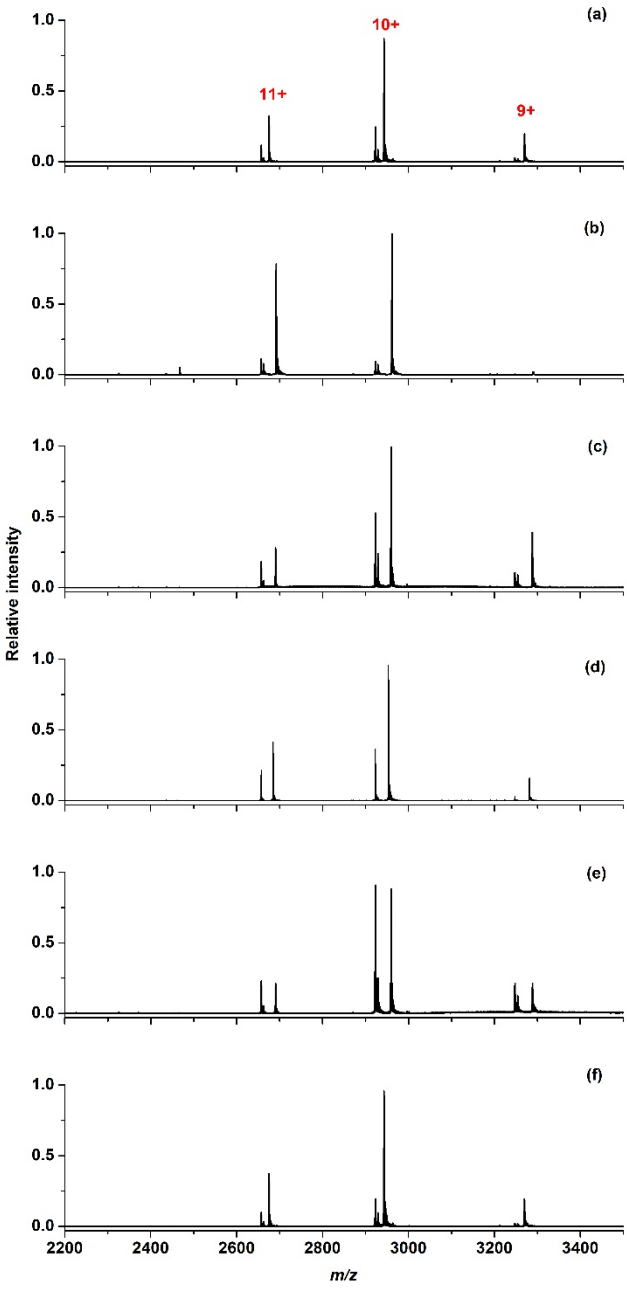

Figure S15. Nanoelectrospray ionization mass spectra of human carbonic anhydrase II and (a) ethoxzolamide, (b) brinzolamide, (c) furosemide, (d) dichlorophenamide, (e) indapamide and (f) acetazolamide in aqueous 70 mM ammonium acetate (pH 7.4) using ~250 nm emitter tips.

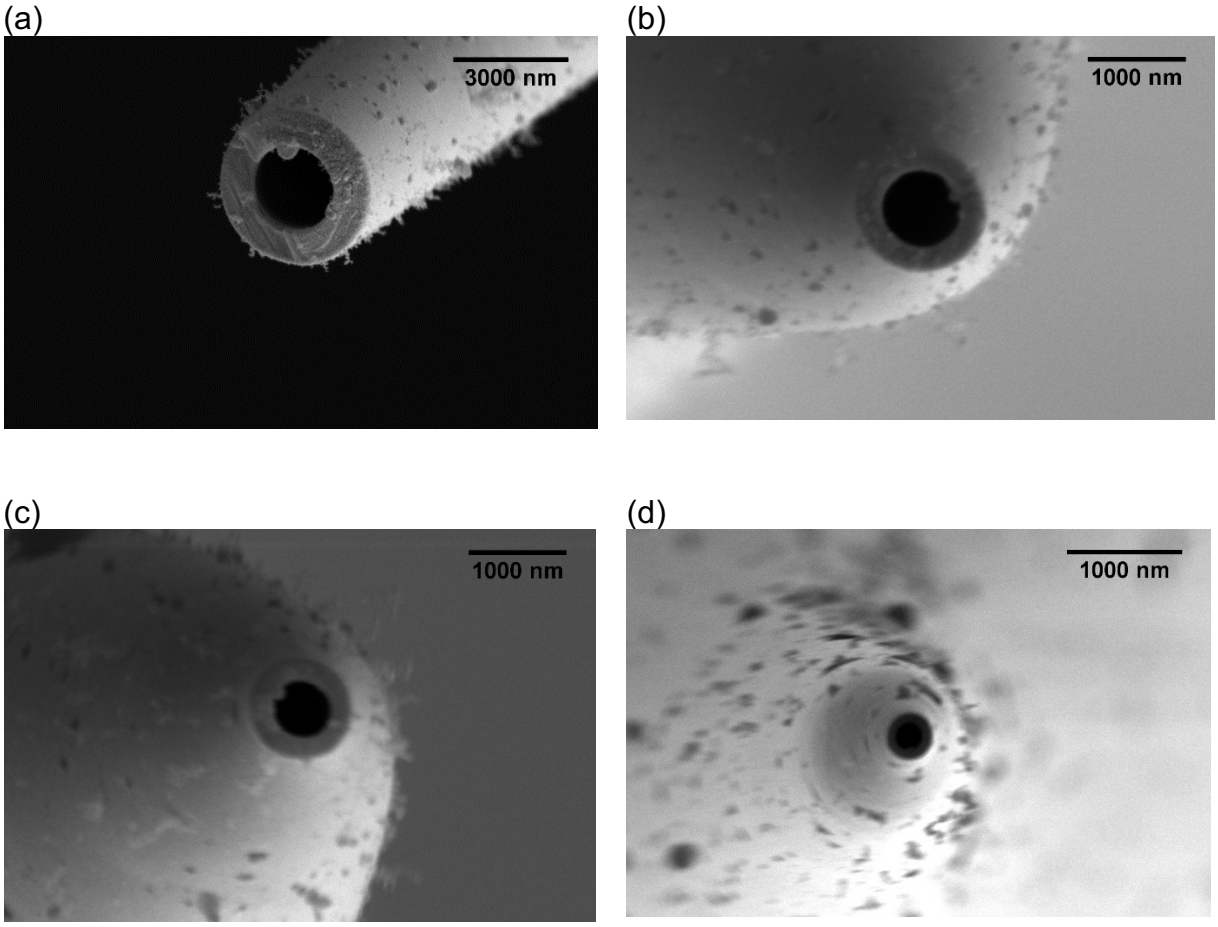

FigureS16. Scanning electron micrographs of the emitters (vertical view) with different openings: (a) ~2000, (b) ~850, (c) ~500, and (d)~250 nm.

References

1. Conroy, C. W.; Maren, T. H., The effect of temperature on the binding of sulfonamides to carbonic anhydrase isoenzymes I, II, and IV. *Mol. Pharmacol.* **1995,** *48* (3), 486-491.
2. Garaj, V.; Puccetti, L.; Fasolis, G.; Winum, J.-Y.; Montero, J.-L.; Scozzafava, A.; Vullo, D.; Innocenti, A.; Supuran, C. T., Carbonic anhydrase inhibitors: novel sulfonamides incorporating 1,3,5-triazine moieties as inhibitors of the cytosolic and tumour-associated carbonic anhydrase isozymes I, II and IX. *Bioorganic Med. Chem. Lett.* **2005,** *15* (12), 3102-3108.
3. Köhler, K.; Hillebrecht, A.; Wischeler, J. S.; Innocenti, A.; Heine, A.; Supuran, C. T.; Klebe, G., Saccharin inhibits carbonic anhydrases: possible explanation for its unpleasant metallic aftertaste. *Angew. Chem., Int. Ed.* **2007,** *46* (40), 7697-7699.
4. Cecchi, A.; Winum, J.-Y.; Innocenti, A.; Vullo, D.; Montero, J.-L.; Scozzafava, A.; Supuran, C. T., Carbonic anhydrase inhibitors: synthesis and inhibition of cytosolic/tumor-associated carbonic anhydrase isozymes I, II, and IX with sulfonamides derived from 4-isothiocyanato-benzolamide. *Bioorganic Med. Chem. Lett.* **2004,** *14* (23), 5775-5780.
5. Imoto, T.; Johnson, L. N.; North, A. C. T.; Phillips, D. C.; Rupley, J. A., 21 vertebrate lysozymes. In *The Enzymes*, Boyer, P. D., Ed. Academic Press: 1972; Vol. 7, pp 665-868.
6. Schindler, M.; Assaf, Y.; Sharon, N.; Chipman, D. M., Mechanism of lysozyme catalysis: role of ground-state strain in subsite D in hen egg-white and human lysozymes. *Biochemistry* **1977,** *16* (3), 423-431.
7. Gavriilidou, A. F. M.; Gülbakan, B.; Zenobi, R., Influence of ammonium acetate concentration on receptor–ligand binding affinities measured by native nano ESI-MS: a systematic study. *Anal. Chem.* **2015,** *87* (20), 10378-10384.
8. Yao, Y.; Shams-Ud-Doha, K.; Daneshfar, R.; Kitova, E. N.; Klassen, J. S., Quantifying protein-carbohydrate interactions using liquid sample desorption electrospray ionization mass spectrometry. *J. Am. Soc. Mass Spectrom.* **2015,** *26* (1), 98-106.
9. Coleman, T.; Wong, S. H.; Podgorski, M. N.; Bruning, J. B.; De Voss, J. J.; Bell, S. G., Cytochrome P450 CYP199A4 from Rhodopseudomonas palustris catalyzes heteroatom dealkylations, sulfoxidation, and amide and cyclic hemiacetal formation. *ACS Catal.* **2018,** *8* (7), 5915-5927.
10. Khalifah, R. G., The carbon dioxide hydration activity of carbonic anhydrase. I. Stop-flow kinetic studies on the native human isoenzymes B and C. *J. Biol. Chem.* **1971,** *246* (8), 2561-2573.
11. Wilkinson, B. L.; Bornaghi, L. F.; Houston, T. A.; Innocenti, A.; Vullo, D.; Supuran, C. T.; Poulsen, S.-A., Carbonic anhydrase inhibitors: inhibition of isozymes I, II, and IX with triazole-linked o-glycosides of benzene sulfonamides. *J. Med. Chem.* **2007,** *50* (7), 1651-1657.
12. Kuwano, Y.; Yoneda, K.; Kawaguchi, Y.; Araki, T., The tertiary structure of an i-type lysozyme isolated from the common orient clam (Meretrix lusoria). *Acta Crystallogr., Sect. F: Struct. Biol. Commun.* **2013,** *69* (Pt 11), 1202-1206.
13. Di Fiore, A.; Pedone, C.; Antel, J.; Waldeck, H.; Witte, A.; Wurl, M.; Scozzafava, A.; Supuran, C. T.; De Simone, G., Carbonic anhydrase inhibitors: the X-ray crystal structure of ethoxzolamide complexed to human isoform II reveals the importance of

thr200 and gln92 for obtaining tight-binding inhibitors. *Bioorganic Med. Chem. Lett.* **2008,** *18* (8), 2669-2674.
14. Bell, S. G.; Yang, W.; Tan, A. B. H.; Zhou, R.; Johnson, E. O. D.; Zhang, A.; Zhou, W.; Rao, Z.; Wong, L.-L., The crystal structures of 4-methoxybenzoate bound CYP199A2 and CYP199A4: structural changes on substrate binding and the identification of an anion binding site. *Dalton Trans.* **2012,** *41* (28), 8703-8714.